Video Article

Kinematic Analysis of Cell Division and Expansion: Quantifying the Cellular Basis of Growth and Sampling Developmental Zones in *Zea mays* Leaves

Katrien Sprangers*[1], Viktoriya Avramova*[1], Gerrit T. S. Beemster[1]

[1]Department of Biology, University of Antwerp

*These authors contributed equally

Correspondence to: Gerrit T. S. Beemster at gerrit.beemster@uantwerpen.be

URL: https://www.jove.com/video/54887
DOI: doi:10.3791/54887

Keywords: Plant Biology, Issue 118, Kinematic analysis, leaf growth, monocotyledonous leaves, maize, cell division, cell expansion, meristem, molecular sampling

Date Published: 12/2/2016

Citation: Sprangers, K., Avramova, V., Beemster, G.T. Kinematic Analysis of Cell Division and Expansion: Quantifying the Cellular Basis of Growth and Sampling Developmental Zones in *Zea mays* Leaves. *J. Vis. Exp.* (118), e54887, doi:10.3791/54887 (2016).

Abstract

Growth analyses are often used in plant science to investigate contrasting genotypes and the effect of environmental conditions. The cellular aspect of these analyses is of crucial importance, because growth is driven by cell division and cell elongation. Kinematic analysis represents a methodology to quantify these two processes. Moreover, this technique is easy to use in non-specialized laboratories. Here, we present a protocol for performing a kinematic analysis in monocotyledonous maize (*Zea mays*) leaves. Two aspects are presented: (1) the quantification of cell division and expansion parameters, and (2) the determination of the location of the developmental zones. This could serve as a basis for sampling design and/or could be useful for data interpretation of biochemical and molecular measurements with high spatial resolution in the leaf growth zone. The growth zone of maize leaves is harvested during steady-state growth. Individual leaves are used for meristem length determination using a DAPI stain and cell-length profiles using DIC microscopy. The protocol is suited for emerged monocotyledonous leaves harvested during steady-state growth, with growth zones spanning at least several centimeters. To improve the understanding of plant growth regulation, data on growth and molecular studies must be combined. Therefore, an important advantage of kinematic analysis is the possibility to correlate changes at the molecular level to well-defined stages of cellular development. Furthermore, it allows for a more focused sampling of specified developmental stages, which is useful in case of limited budget or time.

Video Link

The video component of this article can be found at https://www.jove.com/video/54887/

Introduction

Growth analysis depends on a set of tools that are commonly used by plant scientists to describe genotype determined growth differences and/or phenotypic responses to environmental factors. They include size and weight measurements of the whole plant or an organ and calculations of growth rates to explore the underlying mechanisms of growth. Organ growth is determined by cell division and expansion at the cellular level. Therefore, including the quantification of these two processes in growth analyses is key to understanding differences in whole-organ growth[1]. Consequently, it is crucial to have an appropriate methodology to determine cellular growth parameters that is relatively easy to use by non-specialized laboratories.

Kinematic analysis has already been established as an approach providing a powerful framework for the development of organ growth models[2]. The technique has been optimized for linear systems, such as *Arabidopsis thaliana* roots and monocotyledonous leaves, but also for non-linear systems, such as dicotyledonous leaves[3]. Nowadays, this methodology is increasingly being used to study how genetic, hormonal, developmental, and environmental factors influence cell division and expansion in various organs (**Table 1**). Moreover, it also provides a framework to link cellular processes to their underlying biochemical, molecular, and physiological regulations (**Table 2**), although limitations can be imposed by organ size and spatial organization for techniques that require higher amounts of plant material (*e.g.,* metabolite measurements, proteomics, *etc.*).

Monocotyledonous leaves, such as the maize (*Zea mays*) leaf, represent linear systems in which cells move from the base of the leaf towards the tip, sequentially passing through the meristem and elongation zone to reach the mature zone. This makes it an ideal model system for quantitative studies of the spatial patterns of growth[4]. Moreover, maize leaves have large growth zones (meristem and elongation zone spanning several centimeters[5]) and provide possibilities for studies at other organizational levels. This allows for the investigation of the (putative) regulatory mechanisms controlling cell division and expansion, quantified by kinematic analysis through a range of molecular techniques, physiological measurements, and cell biology approaches (**Table 2**).

Here, we provide a protocol for performing a kinematic analysis in monocot leaves. First, we explain how to conduct a proper analysis of both cell division and cell elongation as a function of position along the leaf axis and how to calculate kinematic parameters. Secondly, we also show how

this can be used as a basis for sampling design. Here, we discuss two cases: high-resolution sampling and focused sampling, enabling improved data interpretation and the saving of time/money, respectively.

Table 1. Overview of kinematic analyses methods for quantification of cell division and expansion in various organs.

organ	reference
monocotyledonous leaves	16, 20, 21, 22
root tips	2, 23, 24, 25, 26, 27, 28, 29
dicotyledonous leaves	21, 30, 31
shoot apical meristem	32

Table 1. Overview of kinematic analyses methods for quantification of cell division and expansion in various organs.

Studies combining spatial quantification of cellular processes by means of kinematic analysis with biochemical, molecular and/or physiological analyses of specific developmental zones

	biochemical/molecular/physiological assays	spatial kinematic parameters	mono/dicotyledonous	species	organ	reference
gene expression	gene expression	cell division	dicotyledonous	*Arabidopsis thaliana*	root	33
		division and expansion rate	dicotyledonous	*Arabidopsis thaliana*	leaf	34
	cell cycle gene expression	division and expansion rate	monocotyledonous	maize (*Zea mays*)	leaf	5
				rice (*Oryza* spp.)	leaf	18
			dicotyledonous	*Arabidopsis thaliana*	leaf	35
						36
						37
	genome wide transcriptome analysis	division and expansion rate	monocotyledonous	maize (*Zea mays*)	leaf	11
						38
			dicotyledonous	*Arabidopsis thaliana*	leaf	39
						40
		expansion rate	monocotyledonous	maize (*Zea mays*)	root	41
	DNA methyltransferases (DMTs) expression	division and expansion rate	monocotyledonous	maize (*Zea mays*)	leaf	42
	gene expression of GA biosynthesis	division and expansion rate	monocotyledonous	maize (*Zea mays*)	leaf	10
	cycB1;2 promoter activity	division and expansion rate	dicotyledonous	*Arabidopsis thaliana*	root	43
proteome	membrane proteome	expansion rate	monocotyledonous	maize (*Zea mays*)	root	44
	phosphoprotein dynamics	leaf elongation rate	monocotyledonous	maize (Zea mays)	leaf	45
metabolite levels	carbohydrates	expansion rate	monocotyledonous	Tall Fescue (*Festuca arundinacea*)	leaf	46
						47
						48
						49
						50
						51
		meristem size and section age	monocotyledonous	Tall Fescue (*Festuca arundinacea*)	leaf	52
						53
	chlorophyll content, H_2O_2, MDA, total antioxidant capacity and antioxidant metabolite levels	division and expansion rate	monocotyledonous	maize (*Zea mays*)	leaf	11
	uronide	expansion rate	monocotyledonous	maize (*Zea mays*)	root	54
	Auxin (IAA), cytokinin (trans Zeatin), Gibberellin (GA 1&4)	division and expansion rate	monocotyledonous	maize (*Zea mays*)	leaf	10
	CDK levels	division and expansion rate	monocotyledonous	maize (*Zea mays*)	leaf	55
	apoplastic peroxide levels	expansion rate	monocotyledonous	maize (*Zea mays*)	root	56
enzyme activity	XET activity	cell expansion	monocotyledonous	soybean (*Glycine max*)	hypocotyl	57
	peroxidase activity	expansion rate	monocotyledonous	Tall Fescue (*Festuca arundinacea*)	leaf	58
						59
	redox regulating enzyme activity	division and expansion rate	monocotyledonous	maize (*Zea mays*)	leaf	11
	CDK activity	division and expansion rate	monocotyledonous	maize (*Zea mays*)	leaf	55
			dicotyledonous	*Arabidopsis thaliana*	root	43
						60
siological measureme	whole growth zone nitrogen content	division and expansion rate	monocotyledonous	*Lolium perenne*	leaf	61
	secondary cell wall depostiong	division and expansion rate	monocotyledonous	Tall Fescue (*Festuca arundinacea*)	leaf	62
	water , dry matter	expansion rate	monocotyledonous	Tall Fescue (*Festuca arundinacea*)	leaf	47
						63
						46
	K, Na, Ca, Mg	expansion rate	monocotyledonous	*Sorghum bicolor*	leaf	22
	nitrogen	expansion rate	monocotyledonous	Tall Fescue (*Festuca arundinacea*)	leaf	64
	respiration rates	meristem size and section age	monocotyledonous	Tall Fescue (*Festuca arundinacea*)	leaf	52
	solute contents, plastic extension, pH	cell length profile	monocotyledonous	maize (*Zea mays*)	leaf	65
	total solutes, K	expansion rate	monocotyledonous	maize (*Zea mays*)	root	66
	total biomass, K and Cl	expansion rate	monocotyledonous	maize (*Zea mays*)	root	67
	apoplastic pH	expansion rate	monocotyledonous	maize (*Zea mays*)	leaf	68
	cell wall dry weight	cell expansion	monocotyledonous	soybean (*Glycine max*)	hypocotyl	57
	turgor	expansion rate	monocotyledonous	maize (Zea mays)	leaf	69
	water potential, osmotic potential, turgor	expansion rate	monocotyledonous	maize (*Zea mays*)	leaf and root	70
cell biology	nuclear ploidy levels	division and expansion rate	monocotyledonous	maize (*Zea mays*)	leaf	5
			dicotyledonous	*Arabidopsis thaliana*	leaf	71
						37
						72
						40
						73
						74
	microtubule arrangement	cell expansion	dicotyledonous	*Arabidopsis thaliana*	root	75
	epidermal development	division and expansion rate	dicotyledonous	*Arabidopsis thaliana*	leaf	39
	nuclear levels, vascular development, stomatal development	division and expansion rate	dicotyledonous	*Arabidopsis thaliana*	leaf	34

Table 2. Link between cellular processes quantified by the kinematic analysis to their regulation at the molecular level. References to various studies linking the quantification of cellular processes to results from biochemical and molecular assays in various species and organs. Xyloglucan endotransglucosylase (XET), malondialdehyde (MDA), cyclin-dependent kinases (CDK). Please click here to view a larger version of this table.

Protocol

NOTE: The following protocol for kinematic analysis is only valid for leaves during steady-state growth. This implies a stable leaf elongation rate and spatial patterns of cell length and expansion in a leaf during a period of several days[6].

1. Plant Growth and Measurements of Leaf Elongation Rate (*LER*)

1. Choose a leaf in steady-state growth and a developmental stage of interest.
   NOTE: There is a difference between steady-state growth and repetitive growth, which implies similar spatial patterns on successive leaves on the same axis. During the early stages of seedling growth, successive leaves typically grow increasingly faster due to the increasing size of the growth zone[7]. Although a few higher leaf positions can have a similar growth pattern[8], this is a transient phase that may be affected by treatments under investigation. It is therefore important to compare lines and treatments strictly on the same leaf position, even though it may be developing at a different time. Even at a constant elongation rate, the growth rate profile is not necessarily the same at different developmental stages. Therefore, it is important to analyze leaves at the same developmental stage[8], typically defined by the number of days after emergence.
2. To perform a full kinematic analysis of leaf growth in monocots, grow at least 15 plants for each treatment and genotype under controlled conditions in a growth room.
3. At the time the leaf of interest appears (emergence from the whorl of surrounding leaves), start measuring the length of the leaf daily with a ruler until the leaf is fully expanded (**Figure 1i**). Leaf length implies the length from soil level to the tip of the leaf. Be careful not to break or damage the leaf, since this might alter its growth.

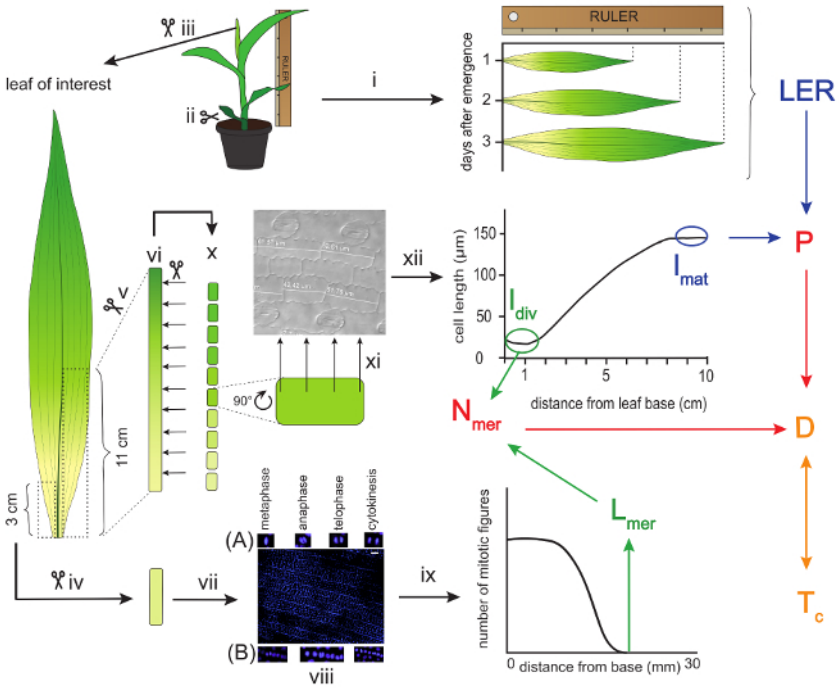

Figure 1: Schematic overview of a kinematic analysis of maize leaves. The leaf of interest is measured with a ruler for three consecutive days to calculate the Leaf Elongation Rate (*LER*). Thereafter, the leaf is harvested and a three-centimeter segment is used for the determination of the meristem size. This is done by measuring the length from the base up to the most distal mitotic figure after DAPI staining. (**A**) Examples of proliferative mitotic figures and (**B**) formative mitotic figures. The first eleven centimeters from the leaf base on the other side of the mid vein are used to cut ten one-centimeter segments for cell length measurements. These measurements provide the basis for creating the cell length profile, which serves to determine the mature cell length (l_{mat}) and the length of cells leaving the meristem (l_{div}). The *LER* and l_{mat} are used to calculate the cell production rate (P), while l_{div} and L_{mer} are used to calculate the number of cells in the meristem (N_{mer}). In turn, P and N_{mer} are used to calculate the average cell division rate (D), which is the inverse of cell cycle duration (T_c). Arrows of the same color indicate parameters that are used to calculate the parameter following on these arrows. Scale bars = 40 µm. Roman numbers are used to refer to specific experimental procedures described in the protocol. Please click here to view a larger version of this figure.

2. Harvesting

1. At the developmental stage of interest (*e.g.,* the third day after emergence), choose at least five representative plants from the batch on which to conduct the kinematic analysis. Continue measuring the rest of the plants as explained in step 1.3 to determine the final leaf length.
2. Cut the above ground part of the plant. To keep the meristematic part intact, cut as close as possible to the roots (**Figure 1ii**).
3. Starting from the outer leaves, remove all leaves up to the leaf of interest by gently unrolling them one by one. If necessary, remove a few extra millimeters from the base to detach the leaves. Also remove the apex and small leaves enclosed by the leaf of interest (**Figure 1iii**).

4. Cut a 3 cm segment, starting from the base on one side of the mid vein, and store it in a 1.5 ml test tube filled with 3:1 (v:v) absolute ethanol:acetic acid solution (CAUTION: wear gloves) at 4 °C for 24 hr up to several months (**Figure 1iv**). This segment will later be used to determine the length of the meristem.
5. From the other side of the vein, cut a 11 cm segment from the base (**Figure 1 v**) and place it in a 15 ml tube filled with absolute ethanol at 4 °C for at least 6 hr to remove pigments (**Figure 1 vi**).
   NOTE: Later on, use only the first 10 cm to determine the cell length profile (see Discussion).
6. Renew the absolute ethanol for another round of cleaning at 4 °C for at least 24 hr (**Figure 1vi**).
7. Finally, substitute the absolute ethanol with pure lactic acid (CAUTION: wear gloves) for cleaning and storage at 4 °C for 24 h or until further use (**Figure 1vi**).

3. Meristem Length Measurements

1. Prepare a rinsing buffer containing 50 mM sodium chloride (NaCl), 5 mM ethylenediaminetetraacetic acid (EDTA; CAUTION: wear gloves) and 10 mM Tris(hydroxymethyl)aminomethane-hydrochloric acid (TRIS-HCl; pH 7).
2. Take the 3 cm segment from section 2.4 and soak it in the buffer for 20 min (**Figure 1vii**).
3. While waiting, use the rinsing buffer to prepare a 4',6-diamidino-2-phenylindole (DAPI) staining solution of 1 µg/ml, keeping it on ice and in the dark.
4. Stain the nuclei by placing the meristem segment for 2-5 min in the DAPI staining solution. Work on ice and in the dark (**Figure 1vii**).
5. Check for fluorescence signal by quickly mounting the segment on a microscopy glass and covering it with a cover glass. The epidermal cells should show fluorescence, while the underlying cell layers should not.
6. If the staining is not sufficient, put the segment back in the DAPI staining solution for some extra minutes.
7. To stop the staining, mount the segments in a drop of rinsing buffer on a microscopy slide and cover with a cover glass.
8. Use a microscope equipped with UV-fluorescence at a 20X magnification, allowing for visualization of around 1,000 epidermal cells at once. Scroll throughout the segment and look for proliferative mitotic figures (metaphase, anaphase, telophase, and cytokinesis), but avoid formative cell division of the developing stomata (**Figure 1viii**)[9]. Define where the most distal mitotic figure is located.
9. Determine the length of the meristem by measuring the distance between the base of the leaf and the most distal epidermal mitotic figure. Use an image-analysis software (*e.g.,* ImageJ) to measure the full length of the image frame.
   1. Count the number of frames that cover the full meristem length (from the leaf base to the most distal mitotic figure) and multiply this number by the length of one frame to obtain the full meristem length (**Figure 1ix**).

4. Cell Length Profile

1. Take the segment that is stored in lactic acid (step 2.5) and place it carefully on the bench. Cut the segments with a scalpel in 10 segments of 1 cm each (**Figure 1x**).
2. Mount the successive leaf segments on a microscopy slide in a small drop of lactic acid. Make sure to consistently face either the adaxial or abaxial side up. In principle, there is no preference for a particular side.
3. Use a microscope equipped with differential interference contrast (DIC) optics to analyze the segments, starting from the leaf base. Measure with an image analysis software the length of at least 20 replicate epidermal cells in files directly adjacent to the stomatal files in order to consistently select the same cell type.
   1. Do this at equally spaced positions along each of the segments (4 positions per segment suffice), and make sure to write down the corresponding position for each measurement throughout the leaf (**Figure 1xi**).
4. Determine the average cell length at each mm along the leaf axis by using a local polynomial smoothing procedure, implemented in an R-script (**Figure 1xii**; Supplementary File 1).
   NOTE: The R-script provides a series of data with increasing smoothing. The amount of smoothing required is somewhat arbitrary and ideally should just remove the local noise, but not affect the overall curve. Make sure to use the same amount of smoothing for all samples within one experiment.
5. Average the cell length at each position between plants and calculate the standard error to create a cell length profile along the leaf axis.

5. Calculations of Kinematic Parameters (See Supplementary File 2)

1. Calculate the *LER* by taking the change in leaf length between two successive time points (*e.g.,* 24 hr, as in step 1.3) and dividing it by the time interval.
2. Calculate the length of the growth zone (L_{gz}) corresponding to the position distal from the base where cells reach 95% of their mature cell length on the smoothened cell length profile.
   1. Take for each position on the smoothened cell length profile 95% of the average of all cell lengths following that position (**Figure 2**).
   2. Compare the smoothened cell lengths (step 4.4) with the calculated 95% cell length at each position. Starting from the base of the leaf, the growth zone ends at the position where the actual cell length equals 95% of the following cell lengths (**Figure 2**; see Supplementary Data 2).

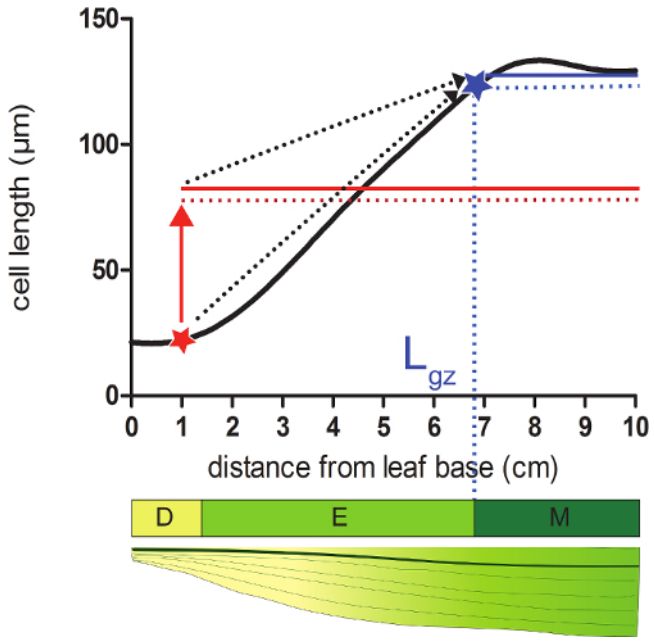

Figure 2: Determining the end of the growth zone. Meristem: At the position indicated with a red star, the actual cell size is smaller than 95% (red dotted line) of the average cell size of all cells following this position (red solid line). The end of the growth zone (L_{gz}; indicated with a blue star) is located where 95% (dotted blue line) of the average cell size of all cells following this position (solid blue line) equals the actual cell size. Division zone (D), elongation zone (E), and mature zone (M). Dashed arrows indicate the convergence between the local size and 95% of the average size over the distal portion of the leaf when moving from the basal positions to the tip of the leaf. Please click here to view a larger version of this figure.

3. Calculate the length of elongation zone (L_{el}) as the difference between the length of the growth zone (L_{gz}) and the meristem size (L_{mer}; determined in step 3).
4. Calculate the mature cell length (l_{mat}) as the average cell length in the mature zone.
5. Divide the *LER* by l_{mat} to obtain the cell production rate (P).
6. Calculate the number of cells in the elongation zone (N_{el}) as the difference between N_{gz} and N_{mer}. The number of cells in the meristem (N_{mer}) equals the cumulative number of cells located in the intervals corresponding to the meristem. The number of cells in the growth zone (N_{gz}) equals the cumulative number of cells located in the intervals corresponding to the growth zone.
7. Calculate the average cell division rate (D) as P/N_{mer}. The cell cycle duration (T_c) equals $\ln(2)/D$.
8. Calculate the time in the elongation zone (T_{el}) by dividing N_{el} by P. The time in the division zone equals $\log_2(N_{mer})*T_c$. The length of cells leaving the meristem (l_{div}) equals the cell length from the smoothened cell length profile at the end of the meristem.
9. Calculate the average cell expansion rate (R_{el}) using following formula: $\ln(l_{mat})-\ln(l_{div})]/T_{el}$.

Representative Results

Here, we show a comparison between well-watered plants (control, 54% soil water content, (SWC)) and plants subjected to drought stress conditions (drought, 34% SWC) in terms of their leaf growth. All plants were grown in a growth chamber under controlled conditions (16 hr day/8 hr night, 25 °C/18 °C day/night, 300-400 $\mu Em^{-2}sec^{-1}$ photosynthetically active radiation (PAR). The drought conditions were established by withholding water until the correct SWC was reached and then further maintained. In a preliminary study, it was defined that the fifth leaf is the first one to emerge and develop under this stress condition. Therefore, it was chosen as the leaf of interest. The final Leaf Length (*LL*) of the drought-stressed plants was 40% lower than the one of the well-watered plants, which was due to a lower *LER* (**Table 3**). To understand the cellular basis of the leaf growth response, we performed a kinematic analysis. Overall, leaf elongation rate is a function of cell production in the meristem and mature cell size determined in the elongation zone (**Figure 3**). Therefore, the shortening of the leaf must be due to effects on one or both of these parameters. Our results show that while the mature cell length (l_{mat}) was not affected, the cell production rate (P) was reduced by 71% (**Table 3**). l_{mat} depends on the length of the cells leaving the meristem (l_{div}), the time these cells spend in the elongation zone (T_{el}), and the relative cell expansion rate (R_{el}). No effect was observed for l_{div}, while R_{el} was reduced by 67% in the drought conditions. This effect was compensated by the almost tripling of T_{el}, which resulted in the same l_{mat} as in the control conditions. The decrease in cell production rate was, in turn, caused by both a lower average cell division rate (D) and a smaller number of cells in the meristem (N_{mer}). Length of the meristem (L_{mer}) was reduced in contrast to the length of the growth zone (L_{gz}), which was not affected significantly. In conclusion, these results show that in this case, cell number, unlike cell size, had a major role in determining leaf size.

Kinematic parameters	C	D	% change C-D	p-value
LL	727±15	436±23	-40	0.000
LER (mm/h)	2.8±0.1	0.8±0.0	-73	0.000
l_{mat} (µm)	140±3	130±6	-7	NS
P (cells/h)	20±1	6±0	-71	0.000
D (cells·cell^{-1}·hr^{-1})	0.028±0.003	0.010±0.001	-63	0.000
T_c (hr)	26±3	71±7	+173	0.000
T_{div} (hr)	249±27	656±71	+164	0.000
L_{mer} (mm)	15±1	11±1	-25	0.010
N_{mer}	740±31	590+20	-20	0.000
R_{el} (µm·µm^{-1}·hr^{-1})	0.043±0.002	0.014±0.001	-67	0.000
l_{div} (µm)	24±2	23±2	-4	NS
T_{el} (hr)	42±2	125±11	+199	0.000
N_{el}	844±54	735±65	-13	NS
L_{gz} (mm)	68±1	61±5	-11	NS
N_{gz}	1584±33	1326±66	-16	0.010

Table 3. Kinematic analysis on cell division and cell expansion during the steady-state growth of the fifth leaf of well-watered plants and plants subjected to drought stress. Data are averages ± SE (n = 5, for *LL*: n = 10). Student's t-test was used as a statistical analysis. Parameters: leaf length (*LL*), leaf elongation rate (*LER*), mature cell length (l_{mat}), cell production rate (*P*), cell division rate (*D*), cell cycle duration (T_c), time in division zone (T_{div}), length of the meristem (L_{mer}), number of cells in the meristem (N_{mer}), relative cell elongation rate (R_{el}), length of the cells leaving the meristem (l_{div}), time in the elongation zone (T_{el}), number of cells in the elongation zone (N_{el}), length of the growth zone (L_{gz}), number of cells in the growth zone (N_{gz}), well-watered conditions (C), drought stress (D), and not significant (NS).

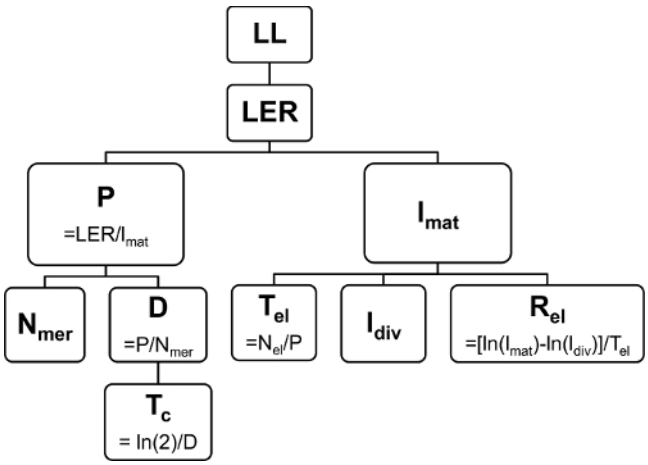

Figure 3: Relationship between the kinematic parameters. The final leaf length (*LL*) depends on the Leaf Elongation Rate (*LER*), which in turn depends on the cell production (*P*) and mature cell length (l_{mat}). The number of cells in the meristem (N_{mer}) and the cell division rate (*D*) together determine *P*, with a cell cycle duration (T_c) as the inverse of *D*. Time in the elongation zone (T_{el}), length of cells leaving the meristem (l_{div}), and the relative cell expansion rate (R_{el}) determine the mature cell length (l_{mat}). The number of cells in the elongation zone (N_{el}). Please click here to view a larger version of this figure.

In addition to its application as a detailed analysis of organ growth, kinematic analysis provides a map of leaf growth zone localization and allows sampling with a subzonal resolution for molecular and biochemical analyses[4,10,11]. As an example, **Figure 4A** shows malondialdehyde (MDA) quantification along the growth zone of the maize leaf in plants subjected to the same conditions as above. MDA is a secondary metabolite formed during lipid peroxidation by ROS and reflects the levels of oxidative damage[12]. MDA was measured in every centimeter of the leaf, starting from its base, which allowed analysis of concentration changes along the growth gradient[11]. As the drought treatment caused 40% leaf shortening, the length of the developmental zones (meristem, elongation zone, and mature zone) in the control plants did not match the length of the same zones in the drought stressed plants (**Figure 4B**). As seen in **Figure 4B**, the meristem in the control plants was around 1.5 cm long, and the elongation zone spanned from 1.5 to 6.8 cm from the leaf base. In the stressed plants, the meristem was localized from 0 to 1.1 cm and the elongation zone from 1.1 to 6.1 cm. MDA levels and the whole growth zone were increased in drought-stressed plants compared to the control treatment. With the help of the kinematic analysis, we could conclude that MDA content was particularly increased in the mature zone for both control and drought treatments. Without knowing the sizes of the developmental zones, we would conclude that, under drought stress, the MDA content increases in an earlier developmental stage than in the control plants, which would be wrong as it does not take into account the shifting of the zones due to the leaf shortening. Therefore, performing kinematic analysis prior to the biochemical measurements was of crucial importance in order to interpret the data correctly.

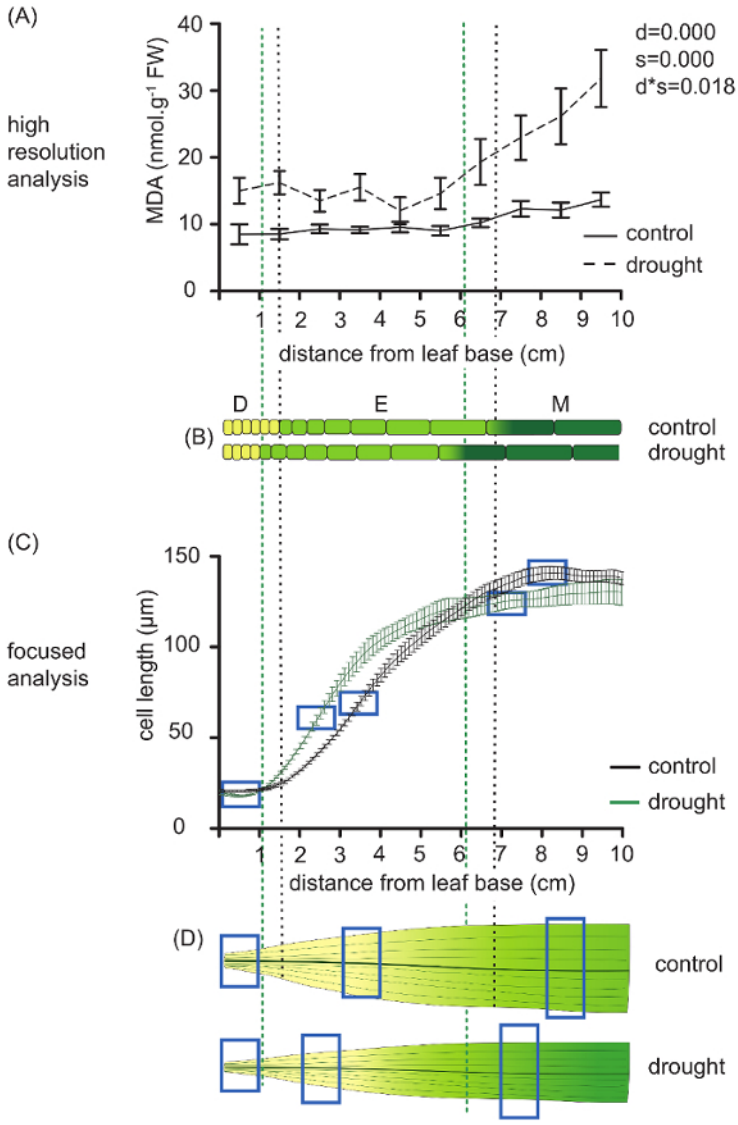

Figure 4: Example of high-resolution biochemical measurements and sampling for focused analysis. (**A**) Malonaldehyde (MDA) concentrations measured along the maize leaf growth zone (divided into ten segments) of plants grown in well-watered condition and plants subjected to drought treatment[10]. Data are averages ± SE (n = 5). Two-way ANOVA was used as a statistical analysis, and p-values are presented next to the graph panel (factors: drought (d) and segment (s)); FW: fresh weight. (**B**) Visualization of the different growth zones in control and drought-stressed plants. Division zone (D), elongation zone (E), and mature zone (M). Cells are magnified 125 times. (**C**) Cell-length profile of control and drought-treated plants. Data are averages ± SE (n = 5). (**D**) Differences in focused sampling in both control and drought-treated plants. The blue boxes indicate sampling position to compare the same developmental stage in both treatments. Please click here to view a larger version of this figure.

In addition to providing the possibility of comparing the same developmental zones in high-resolution studies, the kinematic analysis could also be used as a basis for more focused analyses, in which only samples of specific zones containing cells at the same developmental stage are taken. We compared the cell length profiles, provided by the smoothing of the microscopic cell length measurements, in the first ten centimeters from the leaf base of control and drought-stressed plants. **Figure 4C** shows that, using the cell length profile, we could determine the length of the developmental zones and could also follow the growth rate dynamics in both control and drought-stressed plants. This allowed specific sampling of proliferating cells in the meristem (before the steep increase), expanding cells in the elongation zone (in the middle of the steep increase) and young mature cells in the mature zone (beginning of the plateau). Our results show that, due to the leaf shortening in response to the drought, these zones did not correspond in the control and in the stressed plants. In order to sample proliferating, expanding, and young mature cells in control plants, we needed the first, fifth, and ninth centimeter from the leaf base, respectively. However, in the stressed plants, these segments correspond to the first, fourth, and eighth centimeter, respectively. This kind of more focused sampling has proven to be useful in the case of more laborious, expensive, or time-consuming studies, such as RNA-sequencing, proteomics, metabolomics, *etc.*

Supplementary File 1: R-script for polynomial smoothing procedure. Please right click to download this file.

Supplementary File 2: Calculations of kinematic parameters. Please right click to download this file.

Discussion

A full kinematic analysis on maize leaves enables the determination of the cellular basis of leaf growth and allows for the design of efficient sampling strategies. Although the protocol is relatively straightforward, some caution is recommended in the following critical steps: (1) It is important to detach the younger, enclosed leaves (step 2.3) without damaging the meristem, since meristem length determination (step 3) requires the complete meristem to be present. Some practice beforehand might be needed. (2) Meristematic length determination is based on the interpretation of mitotic figures. Therefore, we advise that, within one experiment, the same person conducts these measurements to reduce variance due to the executor. (3) Even though only ten centimeters is used for the actual cell length measurements, it is important to include eleven centimeters when harvesting the segment for cell length measurements (step 2.5), because the edge of the segment does not always fully submerge in ethanol and/or lactic acid. Therefore, this extra centimeter ensures clearing of the first ten centimeters of the growth zone. (4) In the end, it is useful to inspect the outcome of all kinematic parameters to confirm that they are correct. In **Table 3**, for example, the cell production rate (*P*) of the drought-stressed plants was decreased by 71%, or, in other words, $P_{drought}$ is 0.29 of $P_{control}$. Since the cell production depends on average cell division rate (*D*; -63%) and number of cells in meristem (N_{mer}; -20%; **Figure 3**), the following can be used to validate the output: *P* (0.29) ≈ N_{mer} (0.8) x *D* (0.37). The same can be applied for $LER = P \times I_{mat}$.

Depending on the available facilities, the protocol can be modified in some steps. (1) A more advanced alternative for the daily manual leaf length measurements (step 1.3) is based on Linear Velocity Displacement Transducers (LVDTs)[13]. Its advantage is that it enables measurements at a much higher time resolution, ranging from minutes to seconds. (2) It is crucial to include the complete growth zone during sampling. However, environmental conditions, genotype, species, and the developmental stage examined might alter the length of the growth zone. Therefore, it is useful to make a first estimation of the length of the growth zone in response to your experiment treatment. This protocol is based on the inbred line B73 grown at 25 °C/18 °C (day/night) at 300-400 $\mu Em^{-2}s^{-1}$ (Photosynthetic Active Radiation - PAR). (3) In order to visualize the mitotic figures (step 3.8) without using fluorescence, a Fuelgen stain can be applied[14]. (4) The smoothing of the data can also be done in MS Excel instead of R by using a five-point quadratic fitting with the "Linest" function[15].

An important limitation of this technique is that the whole growth zone needs to be harvested during steady-state growth. In order to ensure steady-state growth, plants must ideally be grown under controlled growth conditions, because fluctuations in light intensity, temperature, or humidity affect the leaf elongation rate[16]. For this reason, the kinematic analysis is less suited for plants grown under field conditions. Another drawback is that leaves need to be emerged, which makes it impossible to examine leaves that are still enclosed by older leaves. Finally, the protocol is suited for monocotyledonous species with large growth zones encompassing at least few centimeters. A kinematic analysis on smaller monocots (*e.g., Poa*, rice), however, is feasible but needs some modifications in the sample preparation[17,18].

Another frequently used approach to analyze differential growth phenotypes is the classical growth analysis. This analysis quantifies whole plant relative growth rates and determines the underlying allocation of photosynthetic derived carbon into a new photosynthetic area and into other parts of the plant[19]. The kinematic analysis, however, allows for a more detailed understanding of the underlying cellular processes that are coupled to growth phenotypes based on quantifying cell division and expansion. Moreover, the possibility to determine the length of each growth zone allows for the correlation of molecular measurements along the leaf axis to the specific developmental stage that is affected by the treatment under study. This is critical for data interpretation. When limited in time or budget or when interested in specific developmental stages, the outcome of this analysis allows for focused sampling, reducing the number of samples needed for analysis. In conclusion, kinematic analysis enables the determination of cellular parameters underlying stress responses and genetic variation in leaf growth and can link them to upstream regulatory processes (**Table 2**).

Disclosures

The authors declare that they have no competing financial interests.

Acknowledgements

This work was supported by a PhD fellowship from the University of Antwerp to V.A.; a PhD fellowship from the Flemish Science Foundation (FWO, 11ZI916N) to K.S.; project grants from the FWO (G0D0514N); a concerted research activity (GOA) research grant, "A Systems Biology Approach of Leaf Morphogenesis" from the research council of the University of Antwerp; and the Interuniversity Attraction Poles (IUAP VII/29,

MARS), "Maize and Arabidopsis Root and Shoot Growth" from the Belgian Federal Science Policy Office (BELSPO) to G.T.S.B. Han Asard, Bulelani L. Sizani and Hamada AbdElgawad all contributed to the video.

References

1. Fiorani, F., & Beemster, G. T. S. Quantitative analyses of cell division in plants. *Plant Mol. Biol.* **60**, 963-979 (2006).
2. Silk, W. K., & Erickson, R. O. Kinematics of Plant-Growth. *J. Theor. Biol.* **76**, 481-501 (1979).
3. Rymen, B., Coppens, F., Dhondt, S., Fiorani, F., & Beemster, G.T.S. Kinematic Analysis of Cell Division and Expansion. In: *Plant Developmental Biology.* L. Hennig & C. Köhler, eds., Chapter 14 (2010).
4. Avramova, V., Sprangers, K., & Beemster, G. T. S. The Maize Leaf: Another Perspective on Growth Regulation. *Trends Plant Sci.* **20**, 787-797 (2015).
5. Rymen, B. *et al.* Cold nights impair leaf growth and cell cycle progression in maize through transcriptional changes of cell cycle genes. *Plant Physiol.* **143**, 1429-1438 (2007).
6. Muller, B., Reymond, M., & Tardieu, F. The elongation rate at the base of a maize leaf shows an invariant pattern during both the steady-state elongation and the establishment of the elongation zone. *J. Exp. Bot.* **52**, 1259-1268 (2001).
7. Beemster, G. T. S., Masle, J., Williamson, R. E., & Farquhar, G. D. Effects of soil resistance to root penetration on leaf expansion in wheat (Triticum aestivum L): Kinematic analysis of leaf elongation. *J. Exp. Bot.* **47**, 1663-1678 (1996).
8. Bernstein, N., Silk, W. K., & Lauchli, A. Growth and Development of Sorghum Leaves under Conditions of Nacl Stress - Spatial and Temporal Aspects of Leaf Growth-Inhibition. *Planta.* **191**, 433-439 (1993).
9. Sylvester, A. W., & Smith, L. G. Cell Biology of Maize Leaf Development. In *Handbook of maize: It's Biology.* Bennetzen, J. L. and Hake S. C., eds., Springer, NY, (2009).
10. Nelissen, H. *et al.* A Local Maximum in Gibberellin Levels Regulates Maize Leaf Growth by Spatial Control of Cell Division. *Curr. Biol.* **22**, 1183-1187 (2012).
11. Avramova, V. *et al.* Drought Induces Distinct Growth Response, Protection, and Recovery Mechanisms in the Maize Leaf Growth Zone. *Plant Physiol.* **169**, 1382-1396 (2015).
12. Picaud, J. C. *et al.* Total malondialdehyde (MDA) concentrations as a marker of lipid peroxidation in all-in-one parenteral nutrition admixtures (APA) used in newborn infants. *Pediatr. Res.* **53**, 406a-406a (2003).
13. Basu, P., Pal, A., Lynch, J. P., & Brown, K. M. A novel image-analysis technique for kinematic study of growth and curvature. *Plant Physiol.* **145**, 305-316 (2007).
14. Van der Weele, C. M. *et al.* A new algorithm for computational image analysis of deformable motion at high spatial and temporal resolution applied to root growth. Roughly uniform elongation in the meristem and also, after an abrupt acceleration, in the elongation zone. *Plant Physiol.* **132**, 1138-1148 (2003).
15. Nelissen, H., Rymen, B., Coppens, F., Dhondt, S., Fiorani, F., & Beemster, G.T.S. In *Plant Organogenesis.* De Smet, I., ed., Chapter 17 (2013).
16. Ben-Haj-Salah, H., & Tardieu, F. Temperature Affects Expansion Rate of Maize Leaves without Change in Spatial-Distribution of Cell Length - Analysis of the Coordination between Cell-Division and Cell Expansion. *Plant Physiol.* **109**, 861-870 (1995).
17. Fiorani, F., Beemster, G. T. S., Bultynck, L., & Lambers, H. Can meristematic activity determine variation in leaf size and elongation rate among four Poa species? A kinematic study. *Plant Physiol.* **124**, 845-855 (2000).
18. Pettko-Szandtner, A. *et al.* Core cell cycle regulatory genes in rice and their expression profiles across the growth zone of the leaf. *J. Plant Res.* **128**, 953-974 (2015).
19. Poorter, H., & Remkes, C. Leaf-Area Ratio and Net Assimilation Rate of 24 Wild-Species Differing in Relative Growth-Rate. *Oecologia.* **83**, 553-559 (1990).
20. Macadam, J. W., Volenec, J. J., & Nelson, C. J. Effects of Nitrogen on Mesophyll Cell-Division and Epidermal-Cell Elongation in Tall Fescue Leaf Blades. *Plant Physiol.* **89**, 549-556 (1989).
21. Tardieu, F., & Granier, C. Quantitative analysis of cell division in leaves: methods, developmental patterns and effects of environmental conditions. *Plant Mol. Biol.* **43**, 555-567 (2000).
22. Bernstein, N., Silk, W. K., & Lauchli, A. Growth and Development of Sorghum Leaves under Conditions of Nacl Stress - Possible Role of Some Mineral Elements in Growth-Inhibition. *Planta.* **196**, 699-705 (1995).
23. Erickson, R. O., & Sax, K. B. Rates of Cell-Division and Cell Elongation in the Growth of the Primary Root of Zea-Mays. *P. Am. Philos. Soc.* **100**, 499-514 (1956).
24. Beemster, G. T. S., & Baskin, T. I. Analysis of cell division and elongation underlying the developmental acceleration of root growth in Arabidopsis thaliana. *Plant Physiol.* **116**, 1515-1526 (1998).
25. Goodwin, R.H., & Stepka, W. Growth and differentiation in the root tip of Phleum pratense. *Am. J. Bot.* **32**, 36-46 (1945).
26. Hejnowicz, Z. Growth and Cell Division in the Apical Meristem of Wheat Roots. *Physiologia Plantarum.* **12**, 124-138 (1959).
27. Gandar, P. W. Growth in Root Apices .1. The Kinematic Description of Growth. *Bot. Gaz.* **144**, 1-10 (1983).
28. Baskin, T. I., Cork, A., Williamson, R. E., & Gorst, J. R. Stunted-Plant-1, a Gene Required for Expansion in Rapidly Elongating but Not in Dividing Cells and Mediating Root-Growth Responses to Applied Cytokinin. *Plant Physiol.* **107**, 233-243 (1995).
29. Sacks, M. M., Silk, W. K., & Burman, P. Effect of water stress on cortical cell division rates within the apical meristem of primary roots of maize. *Plant Physiol.* **114**, 519-527 (1997).
30. Granier, C., & Tardieu, F. Spatial and temporal analyses of expansion and cell cycle in sunflower leaves - A common pattern of development for all zones of a leaf and different leaves of a plant. *Plant Physiol.* **116**, 991-1001 (1998).
31. De Veylder, L. *et al.* Functional analysis of cyclin-dependent kinase inhibitors of Arabidopsis. *Plant Cell.* **13**, 1653-1667 (2001).
32. Kwiatkowska, D. Surface growth at the reproductive shoot apex of Arabidopsis thaliana pin-formed 1 and wild type. *J. Exp. Bot.* **55**, 1021-1032 (2004).
33. Kutschmar, A. *et al.* PSK-alpha promotes root growth in Arabidopsis. *New Phytol.* **181**, 820-831 (2009).
34. Vanneste, S. *et al.* Plant CYCA2s are G2/M regulators that are transcriptionally repressed during differentiation. *Embo J.* **30**, 3430-3441 (2011).
35. Eloy, N. B. *et al.* Functional Analysis of the anaphase-Promoting Complex Subunit 10. *Plant J.* **68**, 553-563 (2011).

36. Eloy, N. B. *et al.* SAMBA, a plant-specific anaphase-promoting complex/cyclosome regulator is involved in early development and A-type cyclin stabilization. *P. Natl. Acad. Sci. USA.* **109**, 13853-13858 (2012).
37. Dhondt, S. *et al.* SHORT-ROOT and SCARECROW Regulate Leaf Growth in Arabidopsis by Stimulating S-Phase Progression of the Cell Cycle. *Plant Physiol.* **154**, 1183-1195 (2010).
38. Baute, J. *et al.* Correlation analysis of the transcriptome of growing leaves with mature leaf parameters in a maize RIL population. *Genome Biol.* **16** (2015).
39. Andriankaja, M. *et al.* Exit from Proliferation during Leaf Development in Arabidopsis thaliana: A Not-So-Gradual Process. *Dev. Cell.* **22**, 64-78 (2012).
40. Beemster, G. T. S. *et al.* Genome-wide analysis of gene expression profiles associated with cell cycle transitions in growing organs of Arabidopsis. *Plant Physiol.* **138**, 734-743 (2005).
41. Spollen, W. G. *et al.* Spatial distribution of transcript changes in the maize primary root elongation zone at low water potential. *Bmc Plant Biol.* **8** (2008).
42. Candaele, J. *et al.* Differential Methylation during Maize Leaf Growth Targets Developmentally Regulated Genes. *Plant Physiol.* **164**, 1350-1364 (2014).
43. West, G., Inze, D., & Beemster, G. T. S. Cell cycle modulation in the response of the primary root of Arabidopsis to salt stress. *Plant Physiol.* **135**, 1050-1058 (2004).
44. Zhang, Z., Voothuluru, P., Yamaguchi, M., Sharp, R. E., & Peck, S. C. Developmental distribution of the plasma membrane-enriched proteome in the maize primary root growth zone. *Front. Plant Sci.* **4** (2013).
45. Bonhomme, L., Valot, B., Tardieu, F., & Zivy, M. Phosphoproteome Dynamics Upon Changes in Plant Water Status Reveal Early Events Associated With Rapid Growth Adjustment in Maize Leaves. *Mol. Cell Proteomics.* **11**, 957-972 (2012).
46. Schnyder, H., & Nelson, C. J. Growth-Rates and Assimilate Partitioning in the Elongation Zone of Tall Fescue Leaf Blades at High and Low Irradiance. *Plant Physiol.* **90**, 1201-1206 (1989).
47. Schnyder, H., Nelson, C. J., & Spollen, W. G. Diurnal Growth of Tall Fescue Leaf Blades .2. Dry-Matter Partitioning and Carbohydrate-Metabolism in the Elongation Zone and Adjacent Expanded Tissue. *Plant Physiol.* **86**, 1077-1083 (1988).
48. Schnyder, H., & Nelson, C. J. Growth-Rates and Carbohydrate Fluxes within the Elongation Zone of Tall Fescue Leaf Blades. *Plant Physiol.* **85**, 548-553 (1987).
49. Vassey, T. L., Shnyder, H. S., Spollen, W. G., & Nelson, C. J. Cellular Characterisation and Fructan Profiles in Expanding Tall Fescue Leaves. *Curr. T. Pl. B.* **4**, 227-229 (1985).
50. Allard, G., & Nelson, C. J. Photosynthate Partitioning in Basal Zones of Tall Fescue Leaf Blades. *Plant Physiol.* **95**, 663-668 (1991).
51. Spollen, W. G., & Nelson, C. J. Response of Fructan to Water-Deficit in Growing Leaves of Tall Fescue. *Plant Physiol.* **106**, 329-336 (1994).
52. Volenec, J. J., & Nelson, C. J. Carbohydrate-Metabolism in Leaf Meristems of Tall Fescue .1. Relationship to Genetically Altered Leaf Elongation Rates. *Plant Physiol.* **74**, 590-594 (1984).
53. Volenec, J. J., & Nelson, C. J. Carbohydrate-Metabolism in Leaf Meristems of Tall Fescue .2. Relationship to Leaf Elongation Rates Modified by Nitrogen-Fertilization. *Plant Physiol.* **74**, 595-600 (1984).
54. Silk, W. K., Walker, R. C., & Labavitch, J. Uronide Deposition Rates in the Primary Root of Zea-Mays. *Plant Physiol.* **74**, 721-726 (1984).
55. Granier, C., Inze, D., & Tardieu, F. Spatial distribution of cell division rate can be deduced from that of p34(cdc2) kinase activity in maize leaves grown at contrasting temperatures and soil water conditions. *Plant Physiol.* **124**, 1393-1402 (2000).
56. Voothuluru, P., & Sharp, R. E. Apoplastic hydrogen peroxide in the growth zone of the maize primary root under water stress.1. Increased levels are specific to the apical region of growth maintenance. *J. Exp. Bot.* **64**, 1223-1233 (2012).
57. Wu, Y. J., Jeong, B. R., Fry, S. C., & Boyer, J. S. Change in XET activities, cell wall extensibility and hypocotyl elongation of soybean seedlings at low water potential. *Planta.* **220**, 593-601 (2005).
58. Macadam, J. W., Nelson, C. J., & Sharp, R. E. Peroxidase-Activity in the Leaf Elongation Zone of Tall Fescue .1. Spatial-Distribution of Ionically Bound Peroxidase-Activity in Genotypes Differing in Length of the Elongation Zone. *Plant Physiol.* **99**, 872-878 (1992).
59. Macadam, J. W., Sharp, R. E., & Nelson, C. J. Peroxidase-Activity in the Leaf Elongation Zone of Tall Fescue .2. Spatial-Distribution of Apoplastic Peroxidase-Activity in Genotypes Differing in Length of the Elongation Zone. *Plant Physiol.* **99**, 879-885 (1992).
60. Beemster, G. T. S., De Vusser, K., De Tavernier, E., De Bock, K., & Inze, D. Variation in growth rate between Arabidopsis ecotypes is correlated with cell division and A-type cyclin-dependent kinase activity. *Plant Physiol.* **129**, 854-864 (2002).
61. Kavanova, M., Lattanzi, F. A., & Schnyder, H. Nitrogen deficiency inhibits leaf blade growth in Lolium perenne by increasing cell cycle duration and decreasing mitotic and post-mitotic growth rates. *Plant Cell Environ.* **31**, 727-737 (2008).
62. Macadam, J. W., & Nelson, C. J. Secondary cell wall deposition causes radial growth of fibre cells in the maturation zone of elongating tall fescue leaf blades. *Ann. Bot-London.* **89**, 89-96 (2002).
63. Schnyder, H., & Nelson, C. J. Diurnal Growth of Tall Fescue Leaf Blades .1. Spatial-Distribution of Growth, Deposition of Water, and Assimilate Import in the Elongation Zone. *Plant Physiol.* **86**, 1070-1076 (1988).
64. Gastal, F., & Nelson, C. J. Nitrogen Use within the Growing Leaf Blade of Tall Fescue. *Plant Physiol.* **105**, 191-197 (1994).
65. Vanvolkenburgh, E., & Boyer, J. S. Inhibitory Effects of Water Deficit on Maize Leaf Elongation. *Plant Physiol.* **77**, 190-194 (1985).
66. Silk, W. K., Hsiao, T. C., Diedenhofen, U., & Matson, C. Spatial Distributions of Potassium, Solutes, and Their Deposition Rates in the Growth Zone of the Primary Corn Root. *Plant Physiol.* **82**, 853-858 (1986).
67. Meiri, A., Silk, W. K., & Lauchli, A. Growth and Deposition of Inorganic Nutrient Elements in Developing Leaves of Zea-Mays L. *Plant Physiol.* **99**, 972-978 (1992).
68. Neves-Piestun, B. G., & Bernstein, N. Salinity-induced inhibition of leaf elongation in maize is not mediated by changes in cell wall acidification capacity. *Plant Physiol.* **125**, 1419-1428 (2001).
69. Bouchabke, O., Tardieu, F., & Simonneau, T. Leaf growth and turgor in growing cells of maize (Zea mays L.) respond to evaporative demand under moderate irrigation but not in water-saturated soil. *Plant Cell Environ.* **29**, 1138-1148 (2006).
70. Westgate, M. E., & Boyer, J. S. Transpiration-Induced and Growth-Induced Water Potentials in Maize. *Plant Physiol.* **74**, 882-889 (1984).
71. Horiguchi, G., Gonzalez, N., Beemster, G. T. S., Inze, D., & Tsukaya, H. Impact of segmental chromosomal duplications on leaf size in the grandifolia-D mutants of Arabidopsis thaliana. *Plant J.* **60**, 122-133 (2009).
72. Fleury, D. *et al.* The Arabidopsis thaliana homolog of yeast BRE1 has a function in cell cycle regulation during early leaf and root growth. *Plant Cell.* **19**, 417-432 (2007).
73. Vlieghe, K. *et al.* The DP-E2F-like gene DEL1 controls the endocycle in Arabidopsis thaliana. *Curr. Biol.* **15**, 59-63 (2005).

74. Boudolf, V. *et al.* The plant-specific cyclin-dependent kinase CDKB1;1 and transcription factor E2Fa-DPa control the balance of mitotically dividing and endoreduplicating cells in Arabidopsis. *Plant Cell.* **16**, 2683-2692 (2004).
75. Baskin, T. I., Beemster, G. T. S., Judy-March, J. E., & Marga, F. Disorganization of cortical microtubules stimulates tangential expansion and reduces the uniformity of cellulose microfibril alignment among cells in the root of Arabidopsis. *Plant Physiol.* **135**, 2279-2290 (2004).